AGU PUBLICATIONS

JGR

Journal of Geophysical Research: Oceans

RESEARCH ARTICLE

10.1002/2015JC011165

Dissipation processes in the Tongue of the Ocean

James A. Hooper V[1,2], Molly O. Baringer[1], Louis C. St. Laurent[3], William K. Dewar[4], and Doug Nowacek[5]

[1]NOAA/AOML/PHOD 4301 Rickenbacker Causeway, Miami, Florida, USA, [2]CIMAS/University of Miami 4600 Rickenbacker Causeway, Miami, Florida, USA, [3]Department of Physical Oceanography, Woods Hole Oceanographic Institution, Woods Hole, Massachusetts, USA, [4]Department of Oceanography, Florida State University, Tallahassee, Florida, USA, [5]Nicholas School of the Environment and Pratt School of Engineering, Duke University Marine Lab, Beaufort, North Carolina, USA

Key Points:
- Large biomass layer shows raised dissipation values between 400 and 600 m
- Biomass shown to be potentially important in the global energy budget

Correspondence to:
J. A. Hooper V,
james.hooper@noaa.gov

Citation:
Hooper, J. A., M. O. Baringer, L. C. St. Laurent, W. K. Dewar, and D. Nowacek (2016), Dissipation processes in the Tongue of the Ocean, *J. Geophys. Res. Oceans*, *121*, 3159–3170, doi:10.1002/2015JC011165.

Received 23 JUL 2015
Accepted 31 MAR 2016
Accepted article online 4 APR 2016
Published online 14 MAY 2016

Abstract The Tongue of the Ocean (TOTO) region located within the Bahamas archipelago is a relatively understudied region in terms of both its biological and physical oceanographic characteristics. A prey-field mapping cruise took place in the fall between 15 September 2008 and 1 October 2008, consisting of a series of transects and "clovers" to study the spatial and temporal variability. The region is characterized by a deep scattering layer (DSL), which is preyed on by nekton that serves as the food for beaked whale and other whale species. This study marks the first of its kind where concurrent measurements of acoustic backscatter and turbulence have been conducted for a nekton scattering layer well below the euphotic zone. Turbulence data collected from a Deep Microstructure Profiler are compared to biological and shear data collected by a 38 kHz Simrad EK 60 echo sounder and a hydrographic Doppler sonar system, respectively. From these measurements, the primary processes responsible for the turbulent production in the TOTO region are assessed. The DSL around 500 m and a surface scattering layer (SSL) are investigated for raised ε values. Strong correlation between turbulence levels and scattering intensity of prey is generally found in the SSL with dissipation levels as large as $\sim 10^{-7}$ W kg^{-1}, 3 orders of magnitude above background levels. In the DSL and during the diel vertical migration, dissipation levels $\sim 10^{-8}$ W kg^{-1} were observed.

1. Introduction

The generation of turbulence in the ocean interior is dependent on the spatial and temporal distribution of physical, topographic, and possibly biological features. Traditionally, turbulence studies have focused on observations in the presence of strong currents or internal waves interacting with rift valleys, canyons, mid-ocean ridges, and open ocean seamounts [*Lueck and Mudge*, 1997; *Polzin et al.*, 1997; *Ledwell et al.*, 2000; *St. Laurent and Thurnherr*, 2007]. Quantifying ocean turbulence is key to understanding the energy sources responsible for sustaining the distribution of water masses in the ocean.

Large-scale mixing experiments involving chemical tracers, as well as vertical microstructure profiler measurements, have observed the average open-ocean mixing value, away from complex topography, is an order of magnitude smaller, i.e., 10^{-5} m^2 s^{-1} [*Ledwell et al.*, 1993; *Toole et al.*, 1994], than Munk's estimate of average diffusivity for the abyssal ocean, 10^{-4} m^2 s^{-1} [*Munk*, 1966]. *Wunsch and Ferrari* [2004] argued that turbulence production caused by tidal interactions with complex topography and by the wind was sufficient to account for the energetic requirements of mixing. However, it is possible that turbulence production at complex topography and by the wind is still insufficient to maintain ocean stratification and may need to be generated through other sources of mechanical energy.

A novel energy source that has received renewed attention is the ocean biosphere, which is the focus of this paper. *Munk* [1966], when considering the energy contribution of the biosphere, determined that the mechanical conversion of chemical energy produced by marine organisms was equivalent in magnitude to the energy produced by tidal dissipation. He estimated that 20% of the chemical energy, approximately 1 TW, was used for swimming, the majority of which occurred in the diel zooplankton migration in the upper 1 km of the ocean. He was focused on the ocean below 1000 m and concluded that in the global budget, biological inputs were of secondary importance.

Dewar et al. [2006] revisited the effect of the marine energy budget and its potential contribution to ocean mixing. Similar to *Munk* [1966], they estimated that approximately 1 TW of the energy produced by net primary production (62.7 TW) was converted to mechanical energy by the kinetic activities of zooplankton and nekton species. This was comparable to the mechanical inputs of both the wind and tides, each of which contributed approximately 1 TW [*Wunsch and Ferrari*, 2004]. *Huntley and Zhou* [2004] also estimated the turbulent dissipation rates of large aggregations of marine animals ranging in size from small krill to whales. They concluded that regardless of the size of the marine animal, the turbulent energy rates produced were between 10^{-5} and 10^{-4} W kg^{-1}. In comparison, wind in the upper 10 m at speeds of between 5 and 20 m s^{-1} produced turbulent dissipation rates up to 2 orders of magnitude less, ranging from 10^{-7} to 10^{-6} W kg^{-1} [*MacKenzie and Leggett*, 1993]. Thus, the biosphere is plausibly just as important an energy source for mixing as the wind and tides.

Recent studies have used microstructure data to examine biologically generated turbulence [*Kunze et al*., 2006; *Gregg and Horne*, 2009]. These studies have focused mainly on the diel vertical migrations of krill in the upper 80 m, as well as aggregations of nekton in the upper 150 m, in coastal inlets and bays. Such migrations form a mobile biomass layer that migrates to the surface at dusk from the "deep" ocean and returns at dawn [*Hays et al*., 2010]. The depth range of these migrations is species dependent; for example, some migrations are as large as 1 km [*Wiebe et al*., 1979; *Heywood*, 1996].

Kunze et al. [2006] observed the diel vertical migrations of krill at a depth of 100 m in Saanich Inlet, British Columbia using an echo sounder to track the biomass through the water column and a tethered microstructure profiler to collect coincident dissipation rates. They observed enhanced turbulent dissipation levels within the detected biomass layer during the vertical migrations were between 10^{-5} and 10^{-4} W kg^{-1}, i.e., 3–4 orders of magnitude above the background level. *Gregg and Horne* [2009] used similar methods to those of *Kunze et al*. [2006] within an aggregation of nekton, most likely of fish origin, in Monterey Bay. They found turbulent dissipation rates between 10^{-6} and 10^{-5} W kg^{-1}, 10–100 times larger during migrations events, down to 90 m.

Previous studies [e.g., *Kunze et al*., 2006; *Gregg and Horne*, 2009] have used colocated measurements of acoustic backscatter and microstructure profiles to measure biologically generated turbulence in the near-surface layer. In contrast, comparable observations for the open ocean deep scattering layer, where most of the zooplankton and other vertically migrating biomass are found, are lacking.

Accordingly, this study takes a first look at the turbulent structure of the deep biomass layers approximately 500 m below the ocean surface. This aggregation of biomass located in the "deep" ocean is known as the deep scattering layer (DSL). The DSL is a dense, permanent biomass layer found within the aphotic zone (often below 400 m), with a vertical thickness of 200–300 m and a horizontal spatial scale of thousands of meters. DSLs are found in nearly all the oceans [*Brekhovskikh and Lysanov*, 2003]. It is possible that the diel vertical migrations from the DSL could play an important role in the transport of gases and nutrients to and from the surface [*Hays*, 2003], in addition to contributing to ocean mixing.

Thus, the objectives of this study are to determine the relative inputs of the DSL during its diel migration to the turbulent dissipation rates observed in the Tongue of the Ocean (TOTO) region (Figure 1) and compare them to other regional, more traditional, sources. The study also addresses the Rothschild-Osborn hypothesis that turbulent dissipation rates produced by velocity shear may influence the contact rates between predator and prey, thus increasing the feeding rate of predators when small-scale turbulence is enhanced. This could, in turn, affect the position of zooplankton in the water column as a means to capture prey or avoid predation [*Rothschild and Osborn*, 1988]. These colocated measurements examine if the same effects are true for the DSL. Furthermore, the mixing levels of the semienclosed TOTO region are compared to the mixing levels of the North Atlantic, an open ocean region. The North Atlantic Tracer Release Experiment (NATRE) [*Ledwell et al*., 1993] location was chosen to study the turbulence of the deep ocean in the general absence of sources of internal wave energy, such as tides and eddies acting along steep topography. As a result, the NATRE data have come to represent the ocean's typical background turbulence.

2. Methods and Data

The Bahamas archipelago (24°15′N, 76°W) is located off the southeast coast of Florida and to the northeast of Cuba (Figure 1). The Atlantic basin extends within the archipelago, forming a deep-sea trough known as

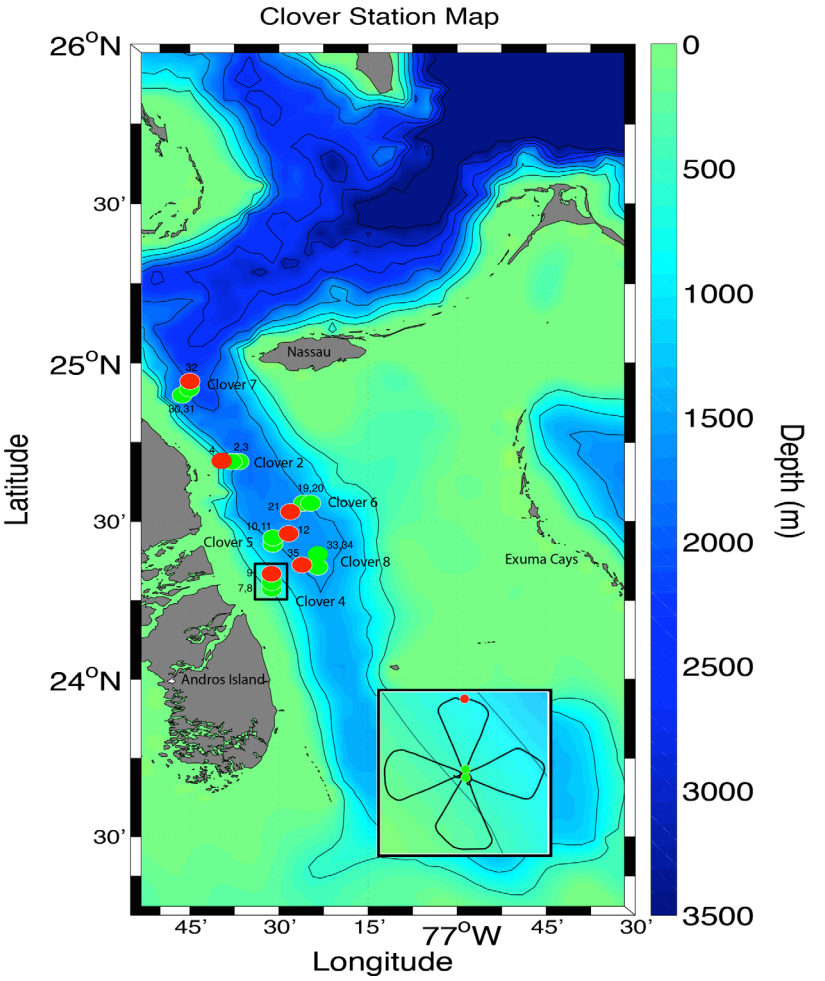

Figure 1. Topography with cruise stations and nominal cruise tracks located in the Tongue of the Ocean. The two center stations (slightly offset for visibility) of each clover are shown in green, with the apex station of each in red. The inset shows a close-up of the clover 4 survey.

the TOTO. The region consists of scattered seamounts with predominantly easterly winds, and the oceanic flow is generally to the northwest the majority of the year [*Smith*, 1995]. The TOTO is sheltered by Andros Island to the west, the Exuma Cays to the east, and Grand Bahamas Banks to the south. The TOTO region is 1500–3600 m deep, 32–64 km wide, and 160 km long [*Schwab et al.*, 1989]. The region is also home to several species of cetaceans, specifically Cuvier's and Blainville's beaked whales, that forage in these sheltered waters [*MacLeod et al.*, 2004]. *Mann and Jarvis* [2004] used Atlantic Undersea Test and Evaluation Center (AUTEC) range hydrophones in the TOTO region to detect what they thought were sounds made by deep-sea fishes at a depth of 500–700 m, the presumed biomass layer exploited by the local cetacean population. However, the TOTO region remains poorly studied in terms of both its biological and physical characteristics, and detailed estimates of the turbulence and characteristics of the DSL have been limited.

A prey-field mapping cruise was conducted over a 2 week period from 15 September 2008 to 1 October 2008 in the TOTO region within the Bahamas archipelago (Figure 1). Biological and physical measurements were taken off the east coast of Andros Island as a series of "clover-leaf" surveys between latitudes 24°N–25°N and longitudes 77°W–78°W. The six clover surveys consisted of 18 microstructure profiles, 3 in each clover, as well as simultaneous measurements of acoustic backscatter and velocity. The profiling strategy consisted primarily of two consecutive profiles taken at the center of each clover with a third taken at the apex of the clover "leaf" (Figure 1). The purpose of the clover track was to capture the temporal and spatial variability of the backscatter field over a scale of 6 km and over the course of 6–8 h using hull-mounted acoustic transducers to examine scale dependence and isotropy. The clovers were taken across the TOTO in

depths ranging from 600 m next to Andros Island to 2000 m in the interior. However, only the upper 800 m was considered in this study, as this is the depth range where the majority of biological activity is observed. Two of the clovers came close to the shelf break on the west coast of Andros Island, with the remaining four clovers taken in the deep interior region. During daylight hours, the ship was committed to numerous small boat operations in support of tagging. We were therefore unable to do sampling during the day. However, three of the clovers were able to start at dusk in an attempt to capture elevated turbulent dissipation rates associated with the diel vertical migration of nekton out of the DSL. The remaining three clovers were conducted during the night postmigration, when the biomass was close to the surface.

The physical measurements obtained from the cruise consisted of temperature, salinity, velocity, shear, and the dissipation rate of turbulent kinetic energy. Three different systems were employed: an autonomous Deep Microstructure Profiler, a 38 kHz Simrad® EK60 echo sounder, and a 50 kHz hydrographic Doppler sonar system (HDSS) mounted to the hull of the R/V *Roger Revelle*. The biological measurements consisted of the depths and densities of the biomass layers obtained from acoustic backscatter intensity. From these measurements, the location and spatial distribution of the biomass layers, as well as the associated physical properties of the TOTO region, were determined. The shear and acoustic backscatter measurements used in comparison with the dissipation profiles were collected while on station (within a 1000 m) and coincide with the time of each dissipation profile. Thus, we were able to obtain turbulent dissipation measurements and examine the processes responsible for the generation of enhanced turbulence dissipation.

During each of the three vertical profiles conducted during each clover survey, centimeter-scale shear microstructure was measured using the Deep Microstructure Profiler (DMP) built by Rockland Scientific International. The DMP is a free-falling, autonomous profiler that measures shear using dual-shear probes. Detailed information about the DMP instrument system can be found online at http://www.rocklandscientific.com. From the shear measurements, estimates of the dissipation rate of turbulent kinetic energy, $\varepsilon = (15/2)\nu <u_z^2>$ (W/kg), were determined, where $\nu = 10^{-6}$ m^2 s^{-1} is the molecular viscosity of seawater and $<uz^2>$ is the mean-square turbulent shear [*Osborn*, 1980]. The shear variance estimates were calculated over 1 m depth intervals using spectral analysis as described by *Gregg* [1999] for each microstructure shear record. Isotropy was assumed [*Yamazaki and Osborn*, 1990] and, typically, the mean of the dual-shear probes was used for each dissipation estimate. The DMP has a dissipation rate noise level of 5–7 $\times$ 10^{-11} W kg^{-1}.

Fine-structure shear data were also obtained from velocity measurements using the hull-mounted HDSS aboard the R/V *Roger Revelle*. The HDSS consists of long-range 50 kHz sonar able to penetrate to depths of 1000 m. The 50 kHz sonar returns profiles with a 9 m binned depth resolution. Detailed information about the HDSS can be found online at http://ieeexplore.ieee.org/xpl/freeabs_all.jsp?arnumber=1194320&abstractAccess=no&userType=inst. The fine-structure shear, Uz, can be used to determine the dynamic stability of the flow, which is governed by the gradient Richardson number, $Ri = N2/(Uz)^2$, where N is the Brunt-Vaisala frequency computed using a least squares fit over 50 m. This represents a competition between the destabilizing effects of shear and the stabilizing effect of buoyancy. If $Ri < 0.25$, the shear layers may become unstable and overturn. Estimates below this critical Ri threshold (i.e., $Ri < 0.25$) on a scale of 10 m are often related to high ϵ measurements, arguing that dynamical instability can cause enhanced oceanic turbulence.

The prey-field measurements were obtained with a Simrad® quantitative echo sounder system. The Simrad® EK60 38-DD transducer (7° beamwidth) was mounted in the transducer tube on the *Revelle* and calibrated before the cruise using standard calibration procedures [*Foote*, 1982]. All acoustic data were collected using 2 kW transmit power with a 2048 s pulse duration and processed in 500 m $\times$ 10 m bins for exploratory analysis. The data were later sorted into 1 m depth bins for fine-scale analyses. Sampling at 38 kHz with this system allowed for the detection of biomass features to depths of up to 2000 m.

The backscattering strength, S_v, is a measure of the concentration of fish in the water column, $S_v = N_f \sigma_{bs}$ (m^{-1}), where N_f is the number of scatterers per unit volume and σ_{bs} is their backscattering cross section. Converting to decibels, $S_v = 20 \log_{10}(s_v)$, where S_v is the volume backscattering strength [*Clay and Medwin*, 1977]. The backscatter is the result of attenuation of active pinging of the water column, and the time lag of the signal S_v from the initial ping can be related to the depth of the scatterers.

3. Results

The backscatter measurements revealed several biological features during the clover surveys (Figure 2). Features such as the seafloor and seamounts, in excess of 1500 m, were resolved. The DSL was a constant feature observed throughout each of the clover surveys. It typically remained around 500 m, with a vertical thickness of 150–200 m, while in the horizontal it spanned the TOTO region where waters are deeper than 1500 m. The volume backscattering strength, S_v, within the DSL typically ranged between −75 and −70 dB in comparison to the background levels of the acoustically quiet waters between −90 and −95 dB (i.e., Figure 3).

The diel vertical migration was represented by a clear gain in volume backscattering strength throughout the water column above the DSL. It was only detected during the dusk profiles (sunset ∼7:05 local) at stations 2, 7, and 10 of clovers 2, 4, and 5 (Figures 2 and 3). The migrating layer ranged in thickness from ∼100 m at station 7 at the beginning of the diel vertical migration (Figure 2a) to spanning the entire water column between the DSL and the surface at stations 2 (i.e., Figure 2b) and 10, although it was concentrated near the surface. The vertical migration elevated the acoustically quiet background levels above the DSL to a S_v ranging from −80 to −70 dB. The S_v observed in the surface scattering layer ranged from −75 dB during the dusk migration period to levels exceeding −70 dB during the night after the migration was complete (Figure 2). We refer the reader to *Hazen et al*. [2011] for a focused treatment of these backscatter measurements.

Starting around 18:30, the DSL began its migration to the surface at station 7 (Figure 2a). There were no elevated dissipation levels observed while passing through the DSL or the areas of elevated backscatter associated with the vertical migration. However, elevated dissipation levels between 10^{-9} and 10^{-8} W kg^{-1} were observed in the acoustically quiet waters starting at a depth of around 250 m up to the surface. At station 2, the elevated backscatter at the end of the migration indicated biomass spread throughout the water column, establishing a well-defined surface scatter layer in the top 100 m (Figure 2b). Elevated dissipation levels were observed within the dispersed diel vertical migration layer, as well as within the DSL between 10^{-9} and 10^{18} W kg^{-1}; there were no bursts of dissipation rates of O(10^{-5} W kg^{-1}) as observed by *Kunze et al*. [2006]. The profile of station 2 passed through a biomass layer more dispersed throughout the water column, which may account for the higher dissipation levels observed in comparison to station 7 (Figure 2b). However, in Figure 2a, the profile at station 7 passed through a well-established, 100 m thick biomass layer during its vertical ascent where minimal dissipation rates of O(10^{-10} W kg^{-1}) were observed. This is consistent with the observations of *Rippeth et al*. [2007] and *Rousseau et al*. [2010] who failed to observe elevated dissipation rates during vertical migration events comparable to *Kunze et al*. [2006]. The low dissipation rates may be a result of the smaller individuals migrating first and the larger individuals migrating later [*Hays et al*., 2010]. Clover 5 started around 19:30, approximately 30 min after sunset, and passed through the biomass near the end of the DVM (clover 5 acoustic time series not shown. Essentially looks like Figure 2b). The biomass had already migrated to the top 200 m where elevated dissipation levels were observed between 10^{-9} and 10^{-8} W kg^{-1} (Figure 3).

Dissipation rates observed during the clover survey shown in Figure 3 exceeded 10^{-8} W kg^{-1}, 2 orders of magnitude above background levels, in 9 out of the 18 profiles (i.e., stations 2, 3, 4, 9, 11, 12, 19, 31, and 33). The majority of elevated dissipation rates were found within the biomass layers. However, we also found elevated dissipation rates within the acoustically quiet waters, suggesting turbulence production in the TOTO region may be a combination of processes, including shear and internal waves, along with the biomass. In the DSL, dissipation rates exceeded 10^{-9} W kg^{-1} in 8 out of the 18 profiles (i.e., stations 2, 3, 4, 11, 12, 31, 34, and 35); dissipation rates exceeding 10^{-8} W kg^{-1} occurred in a subset of just three of these profiles (i.e., stations 2, 3, and 4; Figure 3a). Sustained dissipation rates between 10^{-9} and 10^{-7} W kg^{-1} were observed in the upper 300 m in the surface scattering layer in most of the profiles; 7 of the 18 profiles were greater than 10^{-8} W kg^{-1} (i.e., stations 3, 4, 9, 11, 19, 31, and 33; Figure 3).

Clover 2 demonstrated the most turbulent activity within the DSL, with moderately elevated dissipation rates observed at all three stations between 0.66 and 1.2 × 10^{-8} W kg^{-1} (Figure 3a). The rest of the profiles had observed dissipation rates comparable to background levels between 1 and 36 × 10^{-10} W kg^{-1}. Dissipation rates within the DSL were several orders of magnitude lower than predicted by *Huntley and Zhou* [2004] and those observed by *Gregg and Horne* [2009] in large aggregations of nekton.

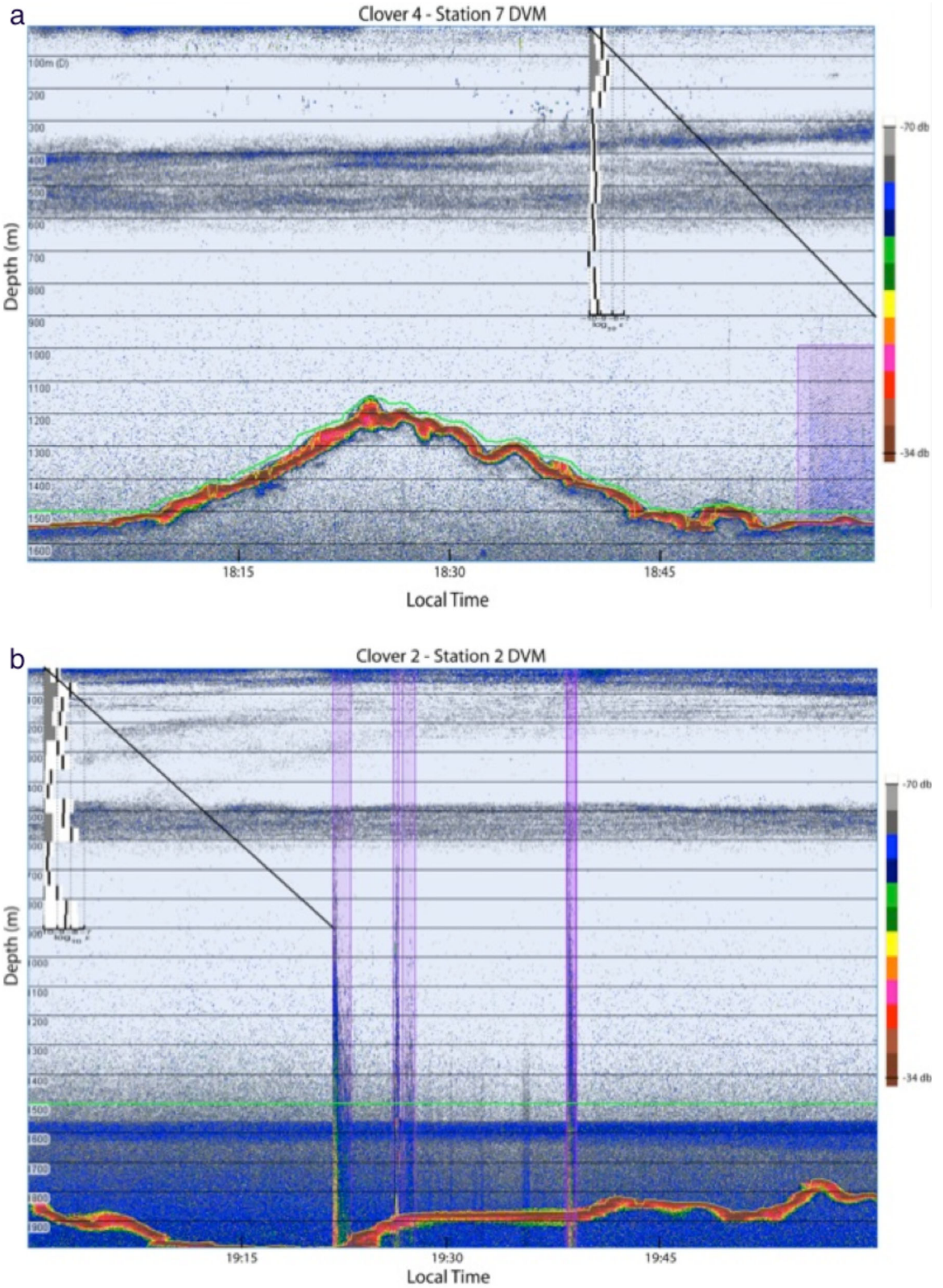

Figure 2. (top) Station 7 from clover 4 and (bottom) station 2 from clover 2 plotted on top of the volume backscattering strength time series. The slanted bold line represents the estimated location of the profile through the water column with time.

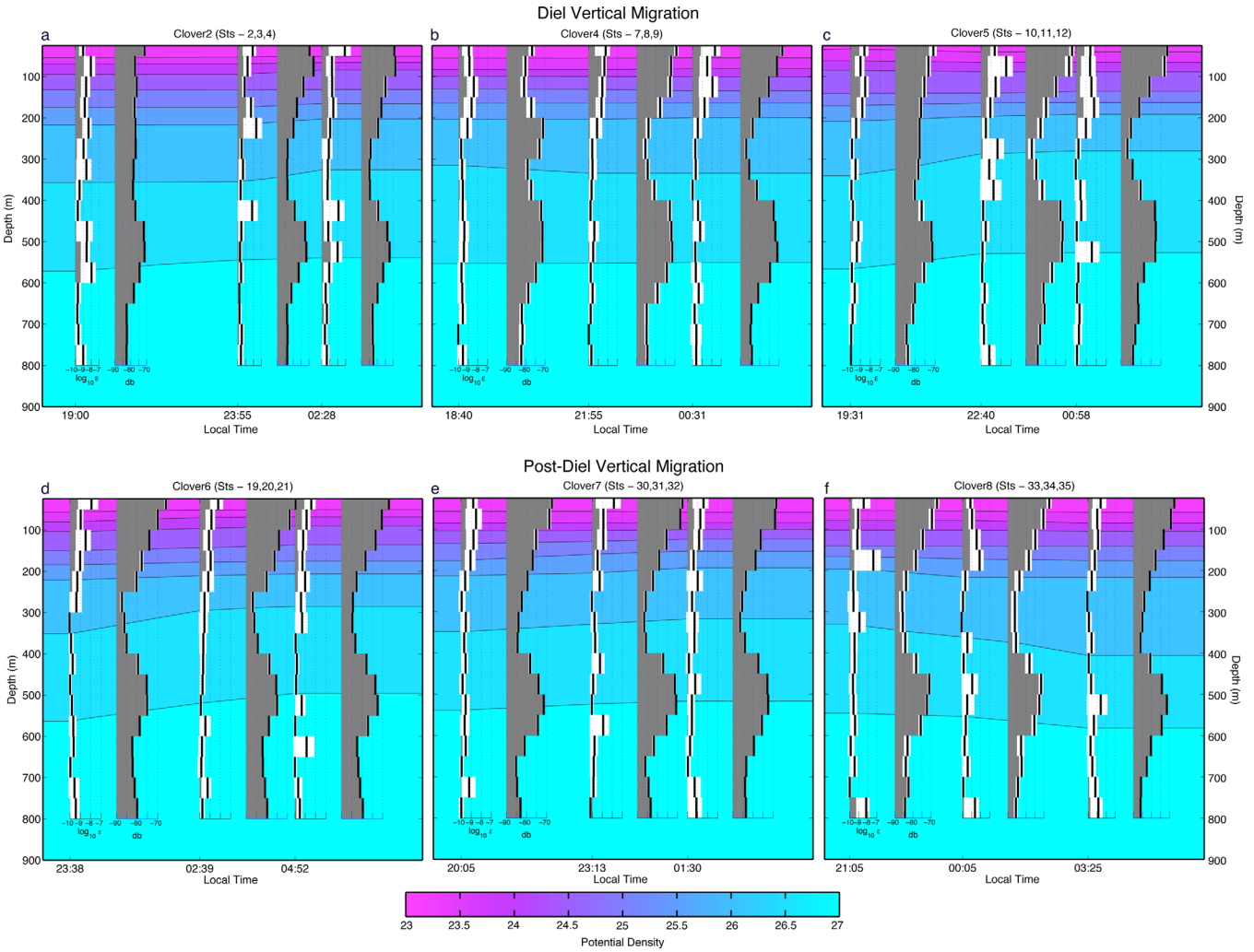

Figure 3. Plot of (top) clovers 2, 4, and 5 conducted during the diel vertical migration and (bottom) clovers 6, 7, and 8 conducted during postdiel vertical migration compared to the dissipation rates and volume backscattering strength with the potential density contours in the background. The profile to the left is the dissipation profile with the acoustic profile to the right in each pair of profiles. The data are estimated over 50 m depth intervals with the bold vertical line representing the mean bin values and the white area the 95% confidence intervals. A logarithmic axis is used for the dissipation data plotted about a reference level of $\varepsilon = 1 \times 10^{-10}$ W kg^{-1}, corresponding to the background dissipation level. The acoustic data are plotted with a reference level of −90 dB.

The magnitude of the shear generated in the TOTO region is shown in Figure 4. The strong shear (red) was predominantly constrained to the surface layer extending down to 200 m and a discrete layer around 800 m (Figure 4). The 200–800 m depth was relatively quiet in terms of fine-structure shear, including where the DSL resided. Clover 8 showed the strongest shear signal in the DSL, but not where the moderate patches of elevated dissipation levels were observed. Clover 4 also showed a moderate shear signal within the DSL; however, no elevated dissipation rates were observed in the DSL at this location. Clovers 2, 5, and 7 showed only weak shear signals in the DSL, although patches of elevated dissipation levels were still observed (Figure 4). Simultaneous fine-structure velocity data and shear microstructure data are not available for clover 6.

The gradient Richardson number, $\mathrm{Ri} = N^2/[U_z]^2$, was calculated to assess the dynamic stability of the water column using 9 m binned velocity shear to calculate the Ri numbers. This will be an underestimation of the velocity shear responsible for small-scale turbulence, but does provide qualitative inferences that have been used in previous studies; for example, *Thurnherr et al.* [2015] showed that large-scale shear estimates can be coherent with in situ dissipation estimates to within a factor of 2. The Ri numbers for the clover surveys seen in Figure 5 are representative of the TOTO region. The critical value, Ri = 0.25, is represented by the blue vertical line; values < 0.25 argue for shear instabilities where elevated dissipation rates can be

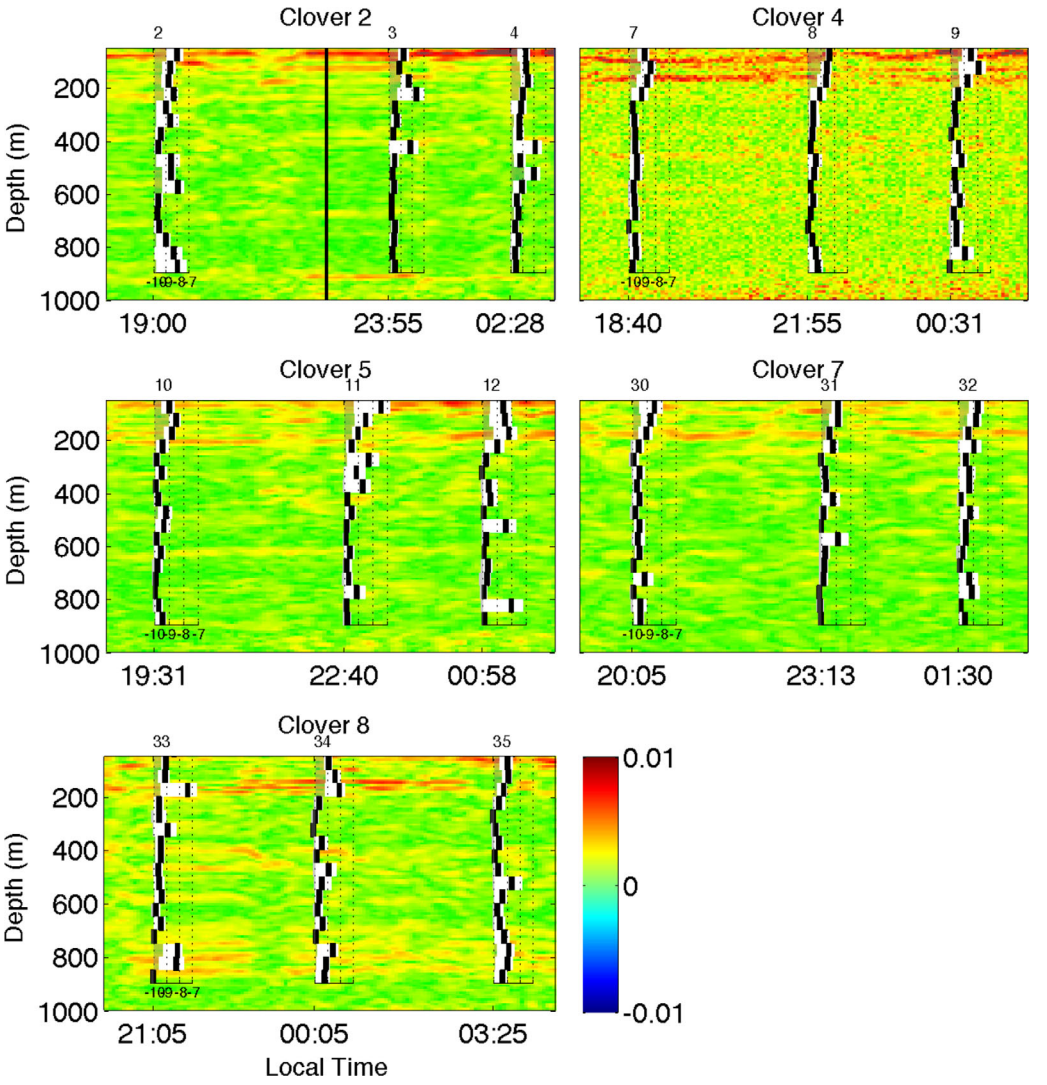

Figure 4. Plot of the clover survey comparing the dissipation profiles plotted on top of the shear magnitude. A logarithmic axis is used for the dissipation data plotted about a reference level of $\varepsilon = 1 \times 10^{-10}$ W kg^{-1}.

expected. Note that with bulk Richardson numbers calculated over relatively large spatial scales several authors have argued that a higher Ri should be used as an indicator of possible turbulence generation through shear instability [e.g., *Baringer and Price*, 1997]. In Figure 5, values below the critical Ri number are observed mainly outside of the DSL, confined to the top 50 m and around 800 m. This suggests the DSL between approximately 400 and 600 m is a dynamically stable region where the generation of intense turbulence associated with shear-induced mixing is not likely to occur.

The correlation coefficients were calculated between the dissipation rates and the volume backscattering strength and between the dissipation rates and the shear (Figure 6). The depth interval of 300–900 m was chosen to eliminate surface influences where multiple processes, such as wind, waves, and biology, may all be contributing to turbulence production. The 95% confidence intervals were calculated using a bootstrap method. Anything above the horizontal blue dotted line represented moderate to strong correlations.

Overall, the dissipation rates were not particularly well correlated with volume backscattering strength and the local shear. The strongest correlation between the dissipation rates and the backscattering strength occurred at the stations sampled during the diel vertical migration. Correlation coefficients of 0.658, 0.711, 0.472, and 0.57 were observed at stations 2, 4, 9, and 10, respectively. It appears as if the presence of the

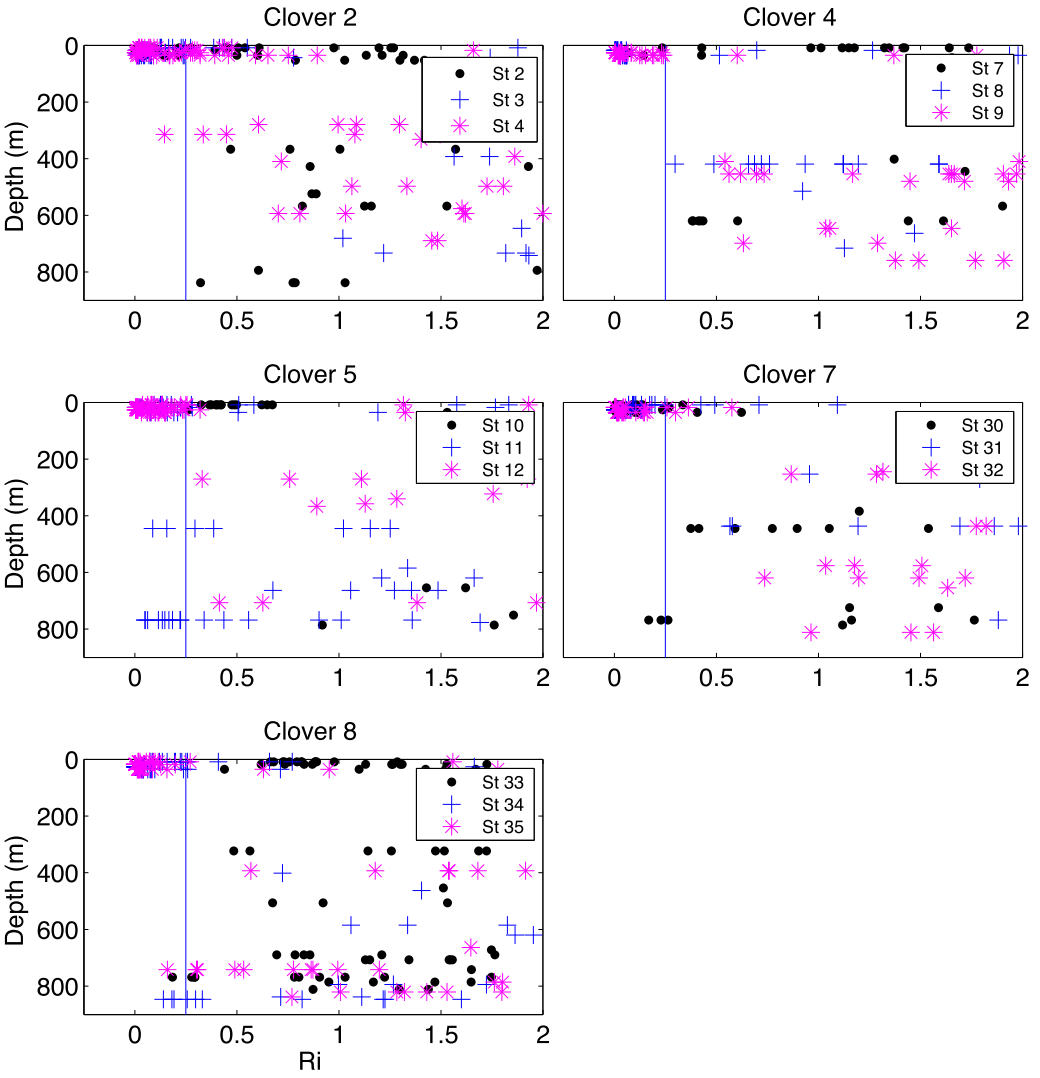

Figure 5. Gradient Richardson number (Ri) for clover survey. The vertical blue line represents the critical Ri number, Ri = 0.25. Points with Ri < 0.25 are areas where shear-produced turbulence is likely.

DVM events is related to the elevated dissipation rates observed. Aside from station 10, at which both shear and acoustic backscatter had a high correlation with dissipation, the strongest correlation with dissipation was seen in the stations conducted after the diel vertical migration. Correlation coefficients of 0.625, 0.646, 0.59, and 0.639 were seen at stations 10, 33, 34, and 35. Clearly, shear also plays an important role in generating dissipation values in the DSL.

The ensemble averages of dissipation rates from the clover survey were compared to those of the NATRE. The NATRE location was chosen to study the turbulence of the deep ocean in the absence of sources of internal wave energy. As a result, the NATRE data represent a prototypical open ocean turbulence state [*Toole et al.*, 1994]. There were four areas seen in the ensemble average of the profiles in the TOTO region where turbulent enhancement was observed (Figure 7). Three of these regions occurred where enhanced shear and low Ri numbers were observed: the surface down to 200 m, a layer between 800 and 1000 m, and near the bottom below 1600 m. Turbulent enhancement at the surface was most likely due to wind and waves, with the possibility of a contribution from the surface scattering layer. The two deeper layers were most likely a result of shear from internal waves breaking and bottom interactions. The fourth layer was between 500 and 700 m where the DSL resided. There was minimal shear observed through this layer, and it is a real possibility that the dissipation rate signal was a result of the DSL.

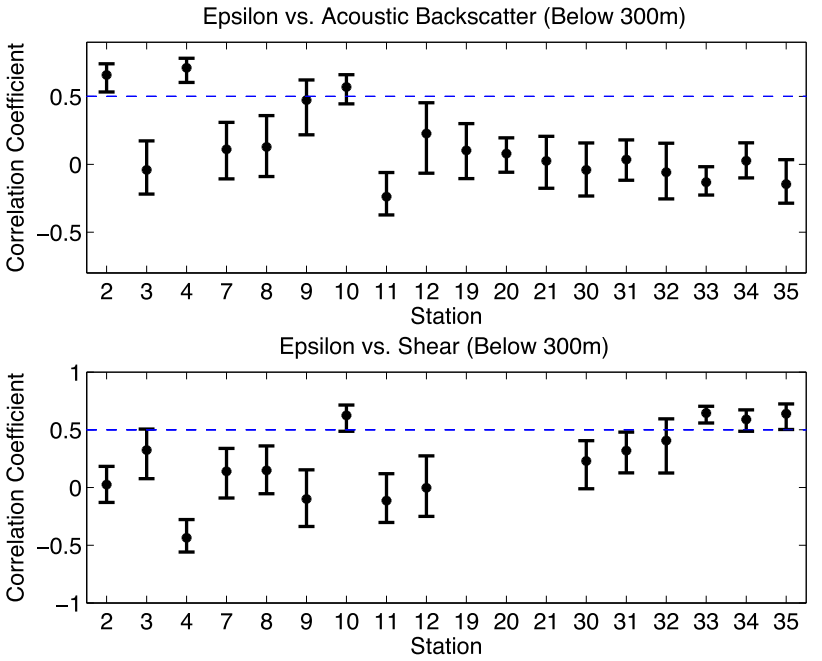

Figure 6. Correlation coefficients between (top) dissipation rates and volume backscattering strength and (bottom) dissipation rates and shear representing profiles below 300 m to eliminate surface signals. The horizontal bars with each dot represent the 95% confidence interval. The blue dotted line at 0.5 represents moderate or better correlations.

4. Discussion

The Rothschild-Osborn hypothesis suggests that in the presence of semipermanent or periodic turbulence some predators or prey adjust their position in the water column as a means to capture prey or avoid predation [*Rothschild and Osborn*, 1988]. It is unlikely that this hypothesis is applicable to the low dissipation rates observed in the DSL, most likely caused by the biomass itself. Without a sustained turbulent motion present, it is unlikely that the turbulence observed in the DSL was used to capture prey or avoid predation. If the Rothschild-Osborn hypothesis was to apply to the DSL, one would expect the coincidence of physical processes responsible for generating turbulence, such as shear, to be more frequent. Our results are more consistent with *Hays et al.* [2010], where it is suggested that the DSL is a sanctuary from predation: prey remains at depth fasting until energy reserves become depleted, forcing them to migrate to the surface under the protection of night to feed. This could explain the lack of energetic local motion within the DSL, resulting in overall low observations of turbulent dissipation rates compared to other studies [e.g., *Kunze et al.*, 2006; *Gregg and Horne*, 2009].

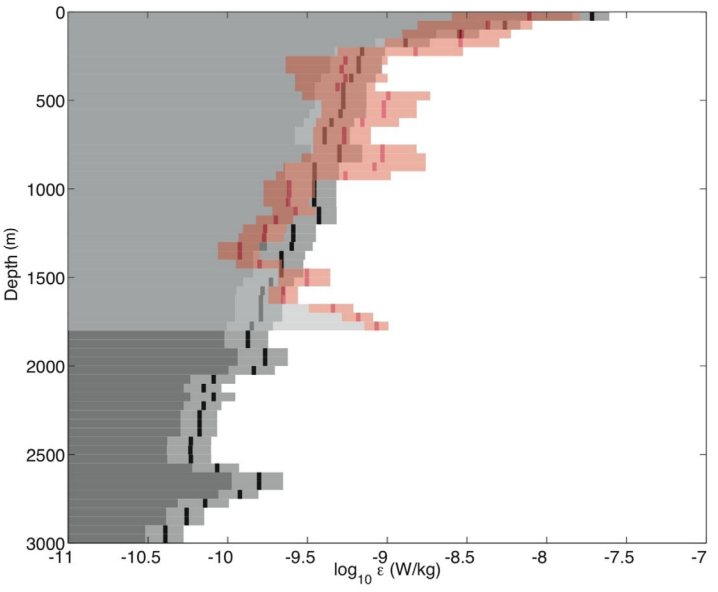

Figure 7. Ensemble average profiles of turbulent dissipation rate estimated from microstructure measurements at two different deep ocean sites: (red) the Tongue of the Ocean Region and (grey) the North Atlantic Tracer Release Experiment. Depth bins of 50 m were used in calculations of the 95% confidence interval (colored bands) and mean (bold vertical lines inside each band).

However, the diel vertical migration can contribute a significant source of turbulence. The correlation coefficients suggest biologically enhanced turbulence in the DSL extending to the surface (Figure 6). During the diel vertical migration, acoustic volume backscatter strength, S_v, approached levels of −70 dB, extending from the DSL to the surface, compared to the background scattering levels of −90 dB. Between the DSL and the surface, dissipation rates were observed at 10–100 times the background level. There were also correlations between the shear and the dissipation levels after the diel vertical migration occurred, with levels reaching 10 times the background dissipation level.

A comparison with the data from the NATRE site suggests the TOTO region was relatively quiet in terms of turbulence production. With average dissipation rates on the order of 1–10 $\times$ 10^{-10} W kg^{-1}, the well-protected waters of the TOTO region appear to be associated with weak fine-structure shear, as suggested by the gradient Richardson number. Turbulence in the TOTO surface layer is likely driven by a combination of biology, wind, and waves, with dissipation rates 10–100 times greater than the deeper background level. Turbulence in the layer around 500 m is likely associated with the DSL whereas, at other depths, physical processes such as shear and internal wave processes likely drive dissipation rates. In all cases where dissipation rates were enhanced in the TOTO region, they seldom exceeded 10 times the background level of 1×10^{-10} W kg^{-1}.

Overall, analysis of the region supports physical processes as the dominant feature driving the moderate turbulence observed with enhancement from the biology. Dissipation rates were never observed in excess of O(10^{-8} W kg^{-1}), as compared to dissipation rates of O($>10^{-5}$ W kg^{-1}) observed in other areas where flow interacted with steep topography [*Lueck and Mudge*, 1997; *St. Laurent and Thurnherr*, 2007] and in large nekton aggregations [*Kunze et al*., 2006; *Gregg and Horne*, 2009]. The DSL appears to produce moderate elevations in dissipation for the most part, but is still highly active twice a day at dusk and dawn during the diel vertical migration. During this period, a significant elevation in turbulence was observed at 100 times the background level. Despite the random and intermittent high levels of turbulence observed, there is evidence to support the DSL and the DVM as possible important contributors. With the DSL being found over most of the Earth's oceans [*Brekhovskikh and Lysanov*, 2003], these vertical migrations could play an interesting role in closing the ocean's energy budget, however, more observations are essential to confirm the magnitude of this intermittent flux.

The DSL is 400–600 m deep and the DVM takes approximately an hour. One microstructure profile takes about 3–4 h to complete for full water column profiles down to 3000 m. In order for future studies to confirm the expected magnitude of DVMs in the earths energy budget, higher temporal and spatial resolution of microstructure profiles are needed to more completely capture activity in the DSL and the DVM events; perhaps a study that specifically focused on profiles to depths just below the DSL would be needed.

Acknowledgments

This research was also carried out in part under the auspices of the Cooperative Institute of Marine and Atmospheric Studies (CIMAS), a Cooperative Institute of the University of Miami, and the National Oceanic and Atmospheric Administration (NOAA), cooperative agreement NA10OAR4320143. Additional support was provided by NOAA/OAR's Atlantic Oceanographic and Meteorological Laboratory. I would also like to thank Rick Lumpkin for his helpful suggestions and Elliot Hazen for his work on the Simrad data. We are grateful for the support of the U.S. Office of Naval Research, specifically award N00014-08-1-1162-01 to Nowacek. Inquiries for the data can be made through the primary author (james.hooper@noaa.gov). We thank the Captain and crew of the R/V Reveille for their support in the field.

References

Baringer, M. O., and J. F. Price (1997), Mixing and spreading of the Mediterranean outflow, *J. Phys. Oceanogr.*, *27*, 8, 1654–1677.

Brekhovskikh, L. M., and Y. P. Lysanov (2003), *Fundamentals of Ocean Acoustics*, AIP Press, N. Y.

Clay, S. C., and H. Medwin (1977), *Acoustical Oceanography: Principles and Applications*, John Wiley, N. Y.

Dewar, W. K., R. J. Bingham, R. L. Iverson, D. P. Nowacek, L. C. St. Laurent, and P. H. Wiebe (2006), Does the marine biosphere mix the ocean?, *J. Mar. Res.*, *64*, 541–561.

Foote, K. (1982), Optimizing copper spheres for precision calibration of hydroacoustic equipment, *J. Acoust. Soc. Am.*, *71*, 742–747.

Gregg, M. C. (1999), Uncertainties and limitations in measuring ϵ and χ, *J. Atmos. Oceanic Technol.*, *16*, 1483–1490.

Gregg, M. C., and J. K. Horne (2009), Turbulence, acoustic backscatter, and pelagic nekton in Monterey Bay, *J. Phys. Oceanogr.*, *39*, 1097–1114.

Hays, G. C. (2003), A review of the adaptive significance and ecosystem consequences of zooplankton diel vertical migrations, *Hydrobiologia*, *503*, 163–170.

Hays, G. C., H. Kennedy, and B. W. Frost (2010), Individual variability in diel vertical migration of a marine copepod: Why some individuals remain at depth when others migrate, *Limnol. Oceanogr.*, *46*, 8, 2050–2054.

Hazen, E. L., D. P. Nowacek, L. St. Laurent, P. N. Halpin, and D. J. Moretti (2011), The relationship among oceanography, prey fields, and beaked whale foraging habitat in the Tongue of the Ocean, *PLoS ONE*, *6*(4), e19269, doi:10.1371/journal.pone.0019269.

Heywood, K. (1996), Diel vertical migration of zooplankton in the northeast Atlantic, *J. Plankton Res.*, *18*(2), 163–184.

Huntley, M. E., and M. Zhou (2004), Influence of animals on turbulence in the sea, *Mar. Ecol. Prog. Ser.*, *273*, 65–79.

Kunze, E., J. F. Dower, I. Beveridge, R. Dewey, and K. P. Bartlett (2006), Observations of biologically generated turbulence in a coastal inlet, *Science*, *313*, 1768–1770.

Ledwell, J. R., A. J. Watson, and C. S. Law (1993), Evidence for slow mixing across the pycnocline from an open-ocean tracer-release experiment, *Nature*, *364*, 701–703.

Ledwell, J. R., E. T. Montgomery, K. L. Polzin, L. C. St. Laurent, R. W. Schmitt, and J. M. Toole (2000), Evidence for enhanced mixing over rough topography in the abyssal ocean, *Nature*, *403*, 179–182.

Lueck, R. G., and T. D. Mudge (1997), Topographically induced mixing around a shallow seamount, *Science*, *276*, 1831–1833.
MacKenzie, B. R., and W. C. Leggett (1993), Wind-based models for estimating the dissipation rates of turbulence energy in aquatic environments: Empirical comparisons, *Mar. Ecol. Prog. Ser.*, *94*, 207–216.
MacLeod, C. D., N. Hauser, and H. Peckham (2004), Diversity, relative density and structure of the cetacean community in summer months east of Great Abaco, Bahamas, *J. Mar. Biol. Assoc. U. K.*, *84*, 469–474.
Mann, D. A., and S. M. Jarvis (2004), Potential sound production by a deep-sea fish, *J. Acoust. Soc. Am.*, *115*(5), 2331.
Munk, W. H. (1966), Abyssal recipes, *Deep Sea Res. Oceanogr. Abstr.*, *13*, 707–730.
Polzin, K. L., J. M. Toole, J. R. Ledwell, and R. W. Schmitt (1997), Spatial variability of turbulent mixing in the abyssal ocean, *Science*, *276*, 93–96.
Rippeth, T. P., J. C. Gascoigne, J. A. M. Green, M. E. Inall, M. R. Palmer, J. H. Simpson, and P. J. Wiles (2007), Turbulent dissipation of coastal seas, edited by Kunze et al., pp. 1768–1770, *Science*.
Rothschild, B. J., and T. R. Osborn (1988), Small-scale turbulence and plankton contact rates, *J. Plankton Res.*, *10*(3), 465–474.
Rousseau, S., E. Kunze, R. Dewey, K. Bartlett, and J. Dower (2010), On turbulence production by swimming marine organisms in the open ocean and coastal waters, *J. Phys. Oceanogr.*, *40*, 2107–2121.
Schwab, W. C., E. Uchupi, R. D. Ballard, and T. K. Dettweiler (1989), Sea-floor observations in the tongue of the ocean, Bahamas: An Argo/SeaMARC survey, *Geo-Mar. Lett.*, *9*, 171–178.
Smith, N. P. (1995), On long-term net flow over Great Bahama Bank, *J. Phys. Oceanogr.*, *25*, 679–684.
St. Laurent, L. C., and A. M. Thurnherr (2007), Intense mixing of lower thermocline water on the crest of the Mid-Atlantic Ridge, *Nature*, *448*, 680–683.
Thurnherr, A. M., E. Kunze, J. M. Toole, L. St. Laurent, K. J. Richards, and A. Ruiz-Angulo (2015), Vertical Kinetic energy and turbulent dissipation in the ocean, *Geophys. Res. Lett.*, *42*, 7639–7647, doi:10.1002/2015GL065043.
Toole, J. M., K. L. Polzin, and R. W. Schmitt (1994), Estimates of diapycnal mixing in the abyssal ocean, *Science*, *264*, 1120–1123.
Wiebe, P. H., L. P. Madin, L. R. Haury, G. R. Harbison, and L. M. Philbin (1979), Diel vertical migration by *Salpa aspera* and its potential for large-scale particulate organic-matter transport to the deep-sea, *Mar. Biol.*, *53*, 249–255.
Wunsch, C., and R. Ferrari (2004), Vertical mixing, energy, and the general circulation of the oceans, *Annu. Rev. Fluid Mech.*, *36*, 281–314.
Yamazaki, H., and T. Osborn (1990), Dissipation estimates for stratified turbulence, *J. Geophys. Rev.*, *95*(C6), 9739–9744, doi:10.1029/JC095iC06p09739.